UCRL-88857
PREPRINT
Conf-8310171--1

A LASER-FUSION ROCKET FOR INTERPLANETARY PROPULSION

Roderick A. Hyde

UCRL--88857

DE84 001238

This paper was prepared for submittal to:
34th International Astronautical Federation
Budapest, Hungary, October 10-17, 1983

September 27, 1983

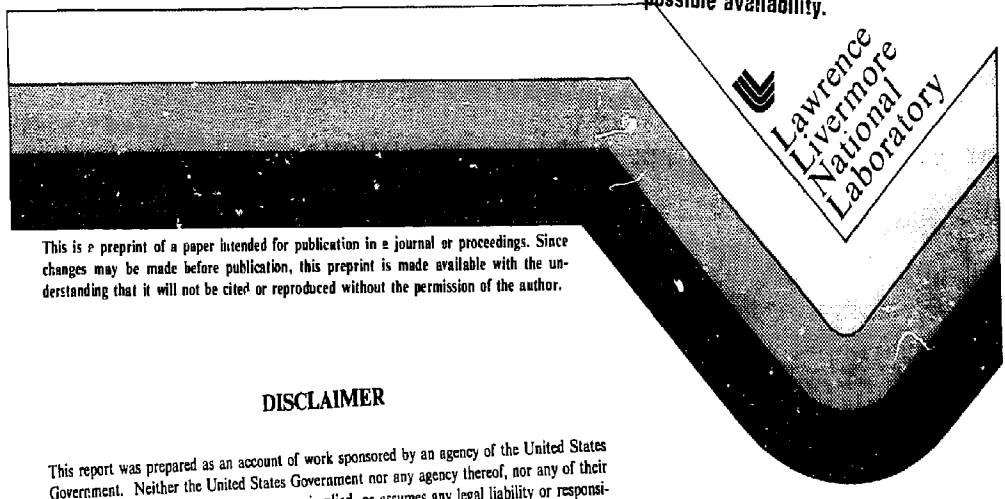

DISCLAIMER

A LASER-FUSION ROCKET FOR INTERPLANETARY PROPULSION

Roderick A. Hyde
Special Studies Group
Lawrence Livermore National Laboratory
Livermore, CA 94550

Abstract

A rocket powered by fusion microexplosions is well suited for quick interplanetary travel. Fusion pellets are sequentially injected into a magnetic thrust chamber. There, focused energy from a fusion "Driver" is used to implode and ignite them. Upon exploding, the plasma debris expands into the surrounding magnetic field and is redirected by it, producing thrust. This paper discusses the desired features and operation of the fusion pellet, its Driver, and magnetic thrust chamber. A rocket design is presented which uses slightly tritium-enriched deuterium as the fusion fuel, a high temperature KrF* laser as the Driver, and a thrust chamber consisting of a single superconducting current loop protected from the pellet by a radiation shield. This rocket can be operated with a power-to-mass ratio of 110 $W\,gm^{-1}$, which permits missions ranging from occasional 9 day "VIP" service to Mars, to routine 1 year, 1500 ton, Plutonian cargo runs.

Introduction

A high performance rocket must have both a large exhaust velocity and a low mass powerplant. Present vehicles lack one or both of these attributes. Nuclear pulsed propulsion[1], permits a rocket to meet both these goals. Nuclear fuel makes it energetically feasible to eject propellent with high exhaust velocity. By burning this fuel explosively, production of energy and thrust can be substantially decoupled from the vehicle. Thus, the rocket operates with a high power-to-mass ratio, combining its fuel-efficient high exhaust velocity with the acceleration required for short trip-times.

The advantages of nuclear pulsed propulsion for space travel have been realized for a long time. Projects initiated in the late 1950's, intended to use small nuclear bombs to propel spaceships. In "Orion", thrust would be produced when the nuclear debris hit a pusher plate, while in "Helios" the explosion was to be contained within a blast chamber, with the propellent expelled through a nozzle. The difficulty faced by these efforts, which ultimately led to their demise, was that they had to use fission energy to drive their explosions. This required fairly large pulse-units, and led to problems concerning the acquisition and subsequent release of fissile material. When lasers were invented, it was very quickly realized that they could, in principle, provide the pulsed power required to initiate small fusion explosions. Since this would avoid both of the difficulties faced by the traditionally-initiated nuclear pulsed propulsion programs, laser-initiated fusion was proposed for use in rockets.[2,3] At the time, however, lasers were clearly incapable of delivering the required amounts of energy and power.

By the start of the 1970's, progress in high power laser and particle beam technology led to the initiation of programs to develop inertial confinement fusion, "ICF", for terrestrial powerplants. It also led to renewed interest in inertial fusion rockets, "IFR"s. Rocket designs were presented[4], which used ICF microexplosions with Orion and Helios style thrust chambers. However, the use of smaller explosions permitted the introduction of magnetic thrust chamber designs[5,6,7]. In these concepts, a fusion pellet is exploded within a magnetic nozzle. As the resultant pellet debris expands, it is controlled by magnetic fields, and expelled by them from the thrust chamber. This produces thrust, while preventing the pellet debris from physically hitting the rocket.

An inertial fusion rocket consists of three major systems: the fusion pellet, the "Driver" which implodes and ignites it, and the thrust chamber that uses the micro-explosion to produce thrust. In this paper, we will discuss the principles behind these systems, and some of the options available in the design of an interplanetary IFR. Accompanying the general discussion, will be the presentation of a particular rocket design. The schematic layout of this vehicle is shown in Fig. 1, and a summary of its mass (using metric tons) in Table 3. This rocket will carry 1500 ton payloads with average trip-times of 6 weeks to Mars, 3 months to Jupiter, and 1 year to Pluto; and allow "VIP" trips lasting less than one half as long.

Fusion Pellet

The energy source which drives an IFR is the fusion pellet, so design of a rocket starts with that of the pellet. The physical processes involved in the implosion and burn of fusion pellets have been recently reviewed.[8,9,10] Basically, energy from a "Driver" is deposited in the outer layers of the pellet. As this outer material is ablated, the inner portions of the pellet are imploded, in a process similar to an inward driving spherical rocket. As the implosion stagnates in a well designed pellet, two conditions are met. There is a large amount of highly compressed fuel - measured by the density-radius product ρr—, and a central portion of the pellet is heated to thermonuclear ignition temperature. As

fuel burns, the energy generated is used to heat and ignite more fuel. Hence, a thermonuclear burn front propagates radially outward through the compressed fuel. Eventually the hot fuel rarefies, quenching the burn. The fraction of fuel burnt prior to this depends on the ρr value achieved by the implosion.

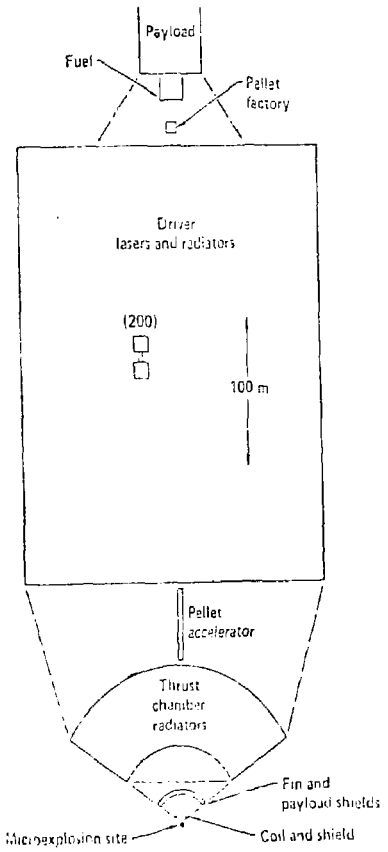

Fig. 1 Vehicle Layout

Three properties of the pellet are of interest in rocket design. The mass of the Driver system is governed by the amount of energy required to implode the pellet. We want pellet designs that maximize the gain, i.e., the ratio of nuclear energy produced to Driver energy required. In addition to the total output of the pellet, we are concerned with its distribution among x-rays, neutrons, and charged particles. The energy deposited in hot plasma can potentially be converted to thrust by a magnetic nozzle. The energy carried by neutrons and x-rays cannot be influenced in this way and will, if intercepted by the thrust chamber, cause vehicle heating. Disposing of this heat with radiators will degrade the rocket's power to mass ratio. Hence there is interest in pellets which deliver most or all of their energy in the form of hot plasma, and little or none of it as neutrons or x-rays. Finally, we must consider the cost of the pellets, which can be governed by the cost and availability of the fuel.

When selecting a fuel, we must consider the following four thermonuclear reactions:

Table 1 Fusion Reactions

D + T	→	He^4 (3.5) + n (14.1)
D + D	→	T (1.01) + p (3.03)
D + D	→	He^3 (0.82) + n (2.45)
D + He^3	→	He^4 (3.67) + p (14.67)

Here, the numbers in parentheses are the product energies in *Mev*. Deuterium is indicated by D, and tritium by T. There are three possible fuels: DD, DT, and DHe^3. The DT reaction ignites at the lowest temperature, and maintains the largest burn rate at all reasonable temperatures. Unfortunately, most of the energy is carried off by an energetic neutron. The two DD reactions burn at similar rates to each other, but their sum is worse in ignition temperature and maximum burn rate than DT. While direct DD burn releases relatively little energy, it produces T and He^3 which promptly burn with another D. The net result in energy per mass is essentially the same for all three fuels. The DHe^3 reaction burns roughly as well as DD; it's harder to ignite but burns faster once lit; both fuels are worse than DT. All the energy from DHe^3 is in the form of charged particles, and is thus potentially useful. Of the three constituents, only D is reasonably inexpensive. It has a cost of $\approx 0.20\ \$\,gm^{-1}$. By contrast, the cost of T is $\approx 7000\ \$\,gm^{-1}$. The standard source of He^3 is currently the decay of T, leading to the same price, although this might be lowered if usefully large lodes of He^4 with above natural He^3 fractions could be mined.

The rocket discussed in this paper uses a pellet containing 15 *mg* of fuel, and detonates 100 pellets per second. The fuel cost is then $0.30\ \$\,sec^{-1}$ with DD fuel, and 6000 $\$\,sec^{-1}$ for DT; DHe^3 may cost somewhat less than DT. This argues very strongly for DD fuel. Nevertheless, the Daedalus study[7] felt that the advantages of DHe^3 were sufficiently compelling to force its use; and in order to obtain an extensive supply proposed mining the Jovian atmosphere. The potential advantage of DHe^3 which can justify the difficulty of obtaining it lies in the absence of non-charged burn products, and hence drastically reduced vehicle heating, rather than in the potential two fold increase in thrust-producing output relative to a DD pellet. However, neither the substantial thrust increase nor the orders of magnitude vehicle heating decrease will actually occur.

Examination of the fusion reactions of Table 1 shows that all four reactions will occur to a significant extent in pellets using any of the three fuels. In particular, DD self-burn within a DHe^3 pellet will account for $\approx 15\%$ of the reactions. Half of these reactions directly produce a neutron, in the other half a T is created, which will promptly burn with another D and hence also produces a neutron. So the difference in reactions and products is only one of degree, with neutron generation differing by less than an order of magnitude between DD and DHe^3 fuels.

Next, note that in order to burn efficiently, the pellets will have a $\rho r \approx 10-20\ gm\ cm^{-2}$. This is larger than the range of the most penetrating neutrons produced in the reactions, which is $\approx 5\ gm\ cm^{-2}$. Hence the energetic neutrons from DD or DT pellets will have their energy largely deposited within the pellet. This reprocessing of neutron energy raises the useful energy fraction of DD and DT pellets, removing the substantial thrust advantage potentially held by DHe^3. But the potential orders of magnitude reduction in harmful energy does not occur either. As mentioned earlier, there are DT reactions within DHe^3 fuel. The 14 *Mev* neutrons produced in these reactions must be stopped if DHe^3 is to hold a massive vehicle heating advantage. But as noted, their scattering distance is $\approx 5\ gm\ cm^{-2}$; a substantial fraction will escape from a pellet before being thermalized. Furthermore, neutrons resulting from either DT or DD burn that are slowed down within the pellet undergo capture by He^3. This reaction yields a T. Even though this capture occurs primarily in the outer regions of the compressed pellet, the high DT burn cross-section insures that most such T will burn. This burn produces a new 14 *Mev* neutron, which starts its escape attempt closer to the edge of the pellet. So the neutrons created from the initial DD reactions will, despite some thermalization, ultimately escape the pellet. While such neutrons will carry off $\approx 2-5\%$ of the energy from a DHe^3 pellet, thereby negating the hoped for orders of magnitude improvement in vehicle heating, there is an even larger source of harmful radiation. At the $\approx 100\ kev$ temperatures at which DD and DHe^3 pellets burn, there is copious production of energetic x-rays due to bremmstrahlung. This occurs regardless of the fuel, and is actually slightly worse for DHe^3 than for DD. For the pellet used in this study, 15% of the energy produced escapes as x-rays.

For the above reasons, I do not foresee a substantial advantage to using DHe^3 fuel in pellets. Accordingly, the economic argument prevails, and DD fuel should be used. However, there is still the difficulty of igniting DD relative to DT. If the Driver is required to light DD, its mass and complexity will escalate drastically. Hence we are compelled to employ some tritium in the pellet in order to facilitate ignition.

In this paper we'll consider a pellet with the characteristics shown in Table 2. About 64% of the energy is released in a useful form. Among the harmful energy-carrying species are γ rays. They are created by (n,γ) reactions, as neutrons leaving the pellet core travel through a high Z tamper which was employed to aid the implosion and to tamp the burning fuel. These γ rays only account for a small fraction of the total pellet energy, but they are penetrating radiation, and will cause shielding problems if superconductors are used in the thrust chamber. We will also be concerned with the amount of tritium used in the pellet. This amounts to $340\ kg\ yr^{-1}$ for a single rocket. By current standards this is a huge amount of T. Inertial fusion rockets will by definition only be used after ICF becomes a reality, so one might assume that T will be acquired from terrestrial ICF reactors. However, this delays the advent of rockets relative to initial ICF success by a time-scale characteristic of the utility industry rather than that of aerospace. The IFR discussed here will be designed to produce its own T; this will be seen to have important implications concerning vehicle heating.

Table 2 Pellet Characteristics

Driver Energy	2 MJ
Peak Power	200 TW
Plasma	1280 MJ
X-Ray	330 MJ
γ-Ray	39 μMole
Neutron	380 MJ
	1.3 mMole
D Used	15 mg
T Used	36 μMole

Thrust Chamber

The primary purpose of the thrust chamber is to convert the energy from ICF pellets into vehicle thrust. In addition to this chore, it must acquire tritium . r use in subsequent pellets, and must generate the power used to operate the fusion Driver.

By virtue of their gain, inertial fusion pellets can serve as an excellent energy source for a rocket. The energy which they produce is much greater than that invested to implode and ignite them. Hence, the Driver technology can have ordinary specific mass characteristics, since the power which it must handle is much less than that generated by the pellet. As long as this energy can be effectively converted into thrust, we can field a very high performance rocket. However, since this conversion system handles the full pellet power, it must do so efficiently and with low specific mass.

It has been recognized for a long time[5,6,7] that the best way to convert ICF energy into thrust is by directly exhausting the pellet debris through a magnetic nozzle. Indirect conversion—such as using the microexplosion to generate electricity which then feeds an ion thruster— inserts systems into the primary power stream which have low specific mass, and whose inefficiencies generate waste heat which must be rejected. As long as the direct mass of the magnetic nozzle can be kept small, it offers much lower specific mass; since it allows power-to-thrust conversion with very little waste heat generation. The useful component of the pellet output, i.e., the hot plasma, dissipates essentially no waste heat in the vehicle during its interaction with it. The magnetic field redirects the plasma without allowing it to directly contact the vehicle. Note that although this conversion process may not be 100% efficient, leaving the plasma exhaust incompletely collimated, the entropy stays in the exhaust stream and does not have to be disposed of by the rocket. If superconductors are used to generate the nozzle fields then the only vehicle heating results from eddy current dissipation during the interaction; this is a small effect. Vehicle

heating due to the harmful portion of the pellet output, i.e., neutrons and x-rays, can be minimized by using a largely transparent structure—one occupying a small fraction of the solid angle as seen from the microexplosion—to generate the magnetic fields of the nozzle. Magnetic nozzles also make the third task of the thrust chamber, the generation of enough power to run the Driver with, trivial through the use of induction coils. As the plasma expands against the magnetic fields of the nozzles, flux changes occur which are readily exploited by induction pickup coils. The electric power collected by the coils is then used to energize the fusion Driver.

Magnetic nozzles allow two of the tasks of the thrust chamber to be fulfilled, while avoiding the waste heat generation which is usually the bane of high exhaust velocity rockets. However, we must still incorporate a tritium acquisition system into our thrust chamber. Tritium will be produced by the following two neutron reactions:

$$n + Li^6 \rightarrow He^4 + T + 4.78\ Mev$$
$$n + Li^7 \rightarrow He^4 + T + n - 2.47\ Mev$$

The primary consequence of this tritium production is that it requires the interception of neutrons from the microexplosion. The Li breeding blanket must handle enough neutrons to ensure production of the 36 μmoles of tritium used in each pellet. In doing so, it will be heated by the incident neutrons, by the accompanying x-rays, and from the heat-of-reaction if the Li^6 process is used. Both reactions should be used, as they access different portions of the pellet's neutron spectrum. The Li^7 reaction has a threshold at 2.47 *Mev*, and is used to convert the unthermalized DT neutrons into tritium. The Li^6 reaction has a high cross-section for thermal neutrons, but charges 4.8 *Mev* per event. Since not using these neutrons will simply force the interception of more solid angle, with the accompanying neutron and x-ray heating, this price is worth paying. In terrestrial fusion reactor designs, breeding ratios, i.e., the ratio of tritium produced to neutrons used, can be greater than one since all neutrons hit the Li blanket. In a rocket blanket which intercepts only a small fraction of the solid angle, the breeding ratio is smaller. Many neutrons enter the Li, elastically scatter, and then depart. As a result, when the blanket-shield geometry used in this study, which is shown in Fig. 2 and will be discussed later, was analyzed with a Monte-Carlo neutronics code, a breeding ratio of only 54% was found. This low breeding ratio drove the required interception fraction from 0.03 to 0.055. The effect of tritium breeding upon the vehicle-heating and hence heat rejection mass, can be seen from multiplying the 710 MJ per pellet energy in neutrons and x-rays by the pellet rep rate of 100 Hz and then by the 0.055 fraction. A 3.0 GW heat load is found, which rises to 4.2 GW when the more accurate neutronics code is used. Not all of this can be charged to the need to breed tritium, since the current carrying structure which produces the nozzle fields will always intercept some solid angle, which can be used to breed tritium. However, the tritium breeding places a floor on vehicle heating; pellets designed for rocket use should use as little tritium as possible.

Let's return to the primary purpose of the thrust chamber, and ask how we can use a magnetic nozzle to convert the expanding pellet debris into thrust. The debris has mass m_p and energy E_K; the maximum possible impulse that can be attained is $\sqrt{2m_pE_K}$. The plasma is a good conductor, and is within the thrust chamber for only a short time. Hence, the magnetic fields of the nozzle do not penetrate the plasma. Instead they induce eddy currents at the boundary of the plasma, and react with it via a $B^2/8\pi$ pressure. As the pellet expands, it sweeps aside the fields of the nozzle. By integrating the PdV work done on the plasma by the nozzle fields during this expansion, and equating it to the energy E_K, we find that the energy stored in the interacting portions of the nozzle magnetic field and of the pellet must be the same. The traditional approach to nozzle design is thus to construct large magnets, which because not all of their field will interact with the pellet, typically must store more field energy than the kinetic energy of the pellet. Before analyzing this type of thrust chamber, let's first consider an alternative approach proposed in the Daedalus study[7] which uses much less stored field energy.

The Daedalus thrust chamber consists of a hemispherical metal shell. The pellet is detonated at the center point. Superconducting coils outside the shell generate a weak magnetic field which fills the volume between the shell and the pellet, but this stored field energy is much smaller than the kinetic energy of the pellet. As the pellet expands, the magnetic flux is trapped between the plasma boundary and the metal shell; so the magnetic field strength, its pressure, and stored energy all rise the closer the plasma comes to the wall. In this approach the field energy which stops and then reflects the plasma, is taken from the kinetic energy of the pellet. There are two advantages to this approach; obviously we save on the mass of the field-generating conductors and their structural supports, but we also can take advantage of the lower field requirements and avoid the use of superconductors. The importance of this will become clear later when we discuss the problem of shielding superconductors from pellet neutrons and γ-rays. There are however two problems with this approach: the shell is not transparent to the pellet, and the thrust conversion efficiency is lower than can be attained with the high field-energy nozzles.

We can solve the first problem by replacing the thin shell by a series of rings, each having a high aspect ratio cross-section and oriented with the long dimension of its cross-section aligned along the line-of-sight to the microexplosion point. The design of this thrust chamber is set by the aspect ratio of the rings; their short dimension is fixed by the conducting skin depth, so the AR determines the long dimension. The inter-ring spacing is limited by this, since in order that the rings be able to cool radiatively they must see open space. The ring spacing and long dimension then bound the closest approach distance of the plasma, as it must not leak out between the rings. The design is then closed by the fact that this approach distance defines the time constant governing the skin depth. With this design, it can be shown that eddy current heating is reduced relative to E_K, by the same factor by which

neutron and x-ray heating is reduced: namely the AR of the rings. The limits on maximum AR are set by the impulsive loading of the rings as pellets are stagnated. The reaction force of the rocket is applied to these rings, and primarily at their tips. In order to avoid crumpling under this loading, it should be oriented along the long axis of the rings, i.e., also along the line-of-sight to the pellet. With this orientation, aspect rations up to $\approx$ 1000 can be used without local buckling of the rings.

This type of thrust chamber acts essentially as a specular reflector of the plasma which it intercepts, and has insufficient field energy to influence the portion of the plasma that is not intercepted. Treating the microexplosion as a point source, we see that the optimum geometry is a paraboloid, not a hemisphere. If we reference the thrust produced to the $\sqrt{2m_pE_K}$ impulse, the efficiency of a paraboloid which subtends angle θ is given by $0.25(1 - \cos\theta)(3 + \cos\theta)$. So a parabolic chamber filling half the solid angle has an efficiency of 75%. Unfortunately, the use of high aspect ratio rings restricts us to a hemispherical shape, since the force vector and pellet line-of-sight must be aligned. A hemisphere has a thrust efficiency of only 50%. The rocket figure-of-merit is power-to-mass, which varies as the square of the thrust conversion coefficient, hence only 25% of the pellet kinetic energy is used. The mass saved by this type of thrust chamber will generally not be enough to offset the loss of exhaust power resulting from its low conversion efficiency.

The rationale behind high field-energy nozzles is that an investment in magnet system mass will be paid back through greater nozzle efficiency. The interaction of the pellet with such nozzles is not however as easy to analyze as it was in the low-energy case. As a result, previous studies[5,6] have simply equated the field energy to that of the plasma. Then, as was also done in the Daedalus case,[7] the thrust efficiency was estimated by assuming the exhaust to be tightly collimated. Half-angles of $\lesssim 20$ degrees were used, yielding exhaust power efficiencies of $\gtrsim 94\%$. This approach proved unreliably optimistic in the low-energy nozzle case, and will undoubtably also be for high-energy nozzles.

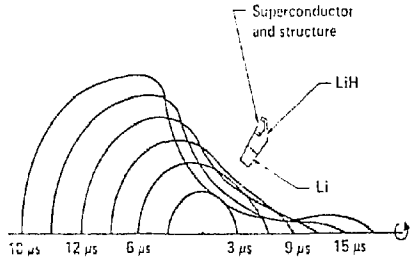

Fig. 2 Pellet in Thrust Chamber

Accordingly, I have calculated the actual nozzle behavior for the system shown in Fig. 2. The field is produced by a single superconducting current loop (the entire geometry is rotationally symmetric about the axis). A radiation shield is placed between the coil and the pellet, protecting the coil from radiation and also serving as the tritium breeding blanket. The shield-coil system is wrapped by a metal skin, which acts as an eddy-current shield during the pellet interaction. As the plasma expands, eddy currents are generated on its surface and on that of the shield-coil. These currents act to prevent field changes within the pellet and the shield-coil. The magnetic $B^2/8\pi$ pressure pushes on the expanding plasma, hopefully collimating the debris as it is expelled from the thrust chamber. A self-consistent calculation was performed by coupling a magnetic field routine, which determined the boundary pressure acting on the plasma as a function of its shape, to a 2D hydrodynamics code which then used this pressure as a boundary condition. The plasma border is shown in Fig. 2 at 6 times during the expansion of an 8.3 gm pellet containing 1300 MJ of kinetic energy. The coil has a radius of 6.5 meters, carries a current of 22 MA, and thus stores five times the kinetic energy of the pellet. This simple coil geometry serves to reflect most of the plasma. As with any axially-symmetric nozzle, a small axial jet is not stopped. A much smaller magnet is used to deflect this jet slightly off-course and above or below the main radiating plane of the rocket. The thrust conversion efficiency of this nozzle, including the negative contribution of the jet, was found to be 65%. Hence it converts 42% of the pellet kinetic energy into exhaust. This larger efficiency allows the rocket to have 68% more powerplant mass than one using the low field-energy type nozzle. As can be seen from Table 3, the mass reduction possible by eliminating the superconductor and its radiation shield is not this large.

As was seen above, the currents which are needed to generate the nozzle magnetic fields are quite large. In our design, this current is carried by a superconductor. Doing so avoids the large power dissipation which would occur with normal conductors, and thereby avoids the resulting heat rejection mass. The mass of the superconductor itself is not large, and is determined by the overall current density at which it operates. The performance of superconductors is degraded in the presence of large magnetic fields. This led us to select a V_3Ga superconductor, which at our 15.8 Tesla peak coil field, and 4.8°K operating temperature, can carry about 270 kA cm^{-2}. For stability reasons, we embed the V_3Ga within a matrix of V and Al, and operate at 85% capacity. The matrix has a net capacity of 42 kA cm^{-2}, which still allows a conductor mass of only 8.7 tons. *In this paper the word "ton" refers to metric ton, i.e., 1 Mg.* This is not however, the only mass associated with the coil. The coil is subjected to a magnetic bursting force, which is resisted in tension by 8.5 tons of structural composite. Even with this addition, our coil stores energy at 375 J gm^{-1}; this is the advantage of using a superconductor.

Unfortunately, the disadvantages of using superconductors in a fusion rocket are almost as compelling. These stem from the need to protect the coil from the microexplosion radiation. Our concern is not material damage; it is the difficulty of heat rejection from a 4.8°K load. The coil is Fig. 2 is directly exposed to $\approx$ 2 GW of neutron and x-ray energy. In order to tolerate the refrigeration mass required to reject waste heat from the coil, we must drop

this by some 6 orders-of-magnitude. It is easy to see that this level of attenuation cannot be reached by using high aspect ratio coils protected by a shadow shield. Some of the neutrons which enter the shield will scatter out of it and enter the coil from its long unprotected side. Hence, as shown in Fig. 2, the radiation shield must extend beyond the line-of-sight, and cover one side of the coil. This has a number of consequences; it increases the subtended cross-section and hence the total heating, it removes the advantage of high aspect ratio coils, and it argues for short *mean-free-path neutron shields. A given coil requirement*, i.e., cross-sectional area and radius, sets a lower bound on intercepted solid angle just because of this shielding difficulty. Either this bound, or the tritium breeding one, will determine the vehicle heating from the pellet; in our present design, the tritium constraint is slightly more stringent. Obviously, the solid angle needed to protect the coil can and should also be used to breed our tritium. The shield of Fig. 2 consists of an inner layer of Li; almost all of the heat is deposited in here, so it can serve both as a tritium breeder and as a heat transfer fluid. The rest of the neutron shield consists of LiH which offers a *smaller mean-free-path than Li. Gamma-rays also prove* to be very troubling, since like the neutrons, they have a small stopping cross-section. Although the number of γ-rays generated by (n,γ) reactions in the pellet and in the radiation shield itself is not large, their presence requires *us to place a massive Pb shield between the coil and the* neutron shield. The thickness of this layer, and of the thermal insulation needed between the coil and shield, further increase the intercepted solid angle. Notice from Fig. 2, that the shields extend around the coil where it can be exposed to reflections from other nearby components of the rocket. Because the shield masses are large, the geometry of Fig. 2 was analyzed using the Monte-Carlo neutron, γ-ray code TARTNP[11]. It was subjected to the pellet neutron and γ-ray spectra, both directly and following reflections from an axial payload radiation shield. The resulting design permits a 2000 watt heat load, and requires *an 8.1 ton refrigerator, with a 44.4 ton neutron shield and* a 56.3 ton γ-ray shield. We see that the shielding requirement has raised the overall coil-related mass to 126 tons, although about 10 tons of this is for Li which would be required as a tritium breeder in any event. Because of the large shielding masses needed to protect against scattered particles, I do not think that multiple superconducting coils should be used in a rocket nozzle.

The shield-coil is not the only massive component of the thrust chamber. A rejection system is needed to dispose of the heat absorbed in the shield. As was mentioned in the tritium breeding discussion, this heat load amounts to 4.2 GW. The heating occurs at the inner portion of the radiation shield, with the x-rays depositing in the metal wall, and the neutrons within the Li blanket. The heat must be removed from the shield and transferred to the radiator arrays shown in Fig. 1. To do this we will take advantage of the excellent heat capacity of Li; it will be pumped through the shield and then sent to the radiators via 8 transfer pipes. This pumping uses 20 MW and is provided by MHD pumps which utilize the thrust chamber magnetic field. The transport to the radiator is also expensive in terms of mass, requiring 27 tons worth of fluid and pipes. At the radiator, the liquid lithium is counterflowed past heat pipes, whose walls constitute the radiating surface. There are 7800 separate heat pipes, each of which is 11 meters long and uses lithium at 1500°K as its working fluid. The heat pipes have a mass of 13 tons, bringing the total heat rejection mass up to 40 tons.

The relative size of the heat rejection and the shield-coil masses leads to another option; namely using a normal conductor instead of a superconductor. The advantage is that the vast bulk of the radiation shield would no longer be needed, the disadvantage of course is the increased conductor and heat rejection mass. A simple tradeoff can be performed between the conductor mass and that of additional heat rejector; decreasing the conductor mass causes the ohmic heating, and hence rejector mass, to increase. The figure of merit for a conductor in this situation is the product of density and resistivity (at the elevated temperature of 1500°K). It turns out that lithium is the best choice, due to its low density. So in this concept, the coil would consist of an annular vat of Li: which would serve as tritium breeder, field generating conductor, and *heat transfer fluid. For our present design parameters*, this type of thrust chamber requires $\approx$ 40 tons more than the baseline system; the reason being that the coil bursting force must now be resisted by a high temperature material. Accordingly, the superconducting coil is used as the baseline system for this paper. However, the Li option should be considered in further studies, for the following reasons. It should be used for low field-energy nozzles where the current needs are lower. It can be used for multiple coil high field-energy nozzles, since we are not concerned with shielding from multiply scattered neutrons. The potential gains in nozzle efficiency may well offset the increased *thrust chamber mass caused by using Li and by inter-coil* forces. Finally, large high-field superconducting magnets are an expensive high-tech item; the simplicity of a normal conductor is attractive.

Fusion Driver

In order to implode and ignite an inertial fusion pellet, a fast acting energy source is required; in our case 2 MJ within 10 nanoseconds. Delivering this energy and power to a small target is not an easy task. To date, both the financial and temporal cost of ICF research have been dominated by Driver development. As a practical matter, early rocket developers will not attempt to duplicate this effort. There will be large and clear advantages in using Drivers developed for terrestrial ICF in inertial fusion rockets.

Unfortunately, the features needed for a good IFR Driver are not the same as those desired in an ICF powerplant Driver. A powerplant Driver must be efficient and inexpensive. While desirable, neither of these features are essential for an IFR Driver. The primary concern in a rocket is the mass associated with the Driver. The first

component of M_{DS} is the direct mass of the Driver, which may have little correlation with its cost. The other Driver related mass is that of its waste heat rejection system. Since radiators will be required, we want a Driver with large ηT^4, which is a much different goal than the large η sought for terrestrial Drivers. A secondary difference between rockets and powerplants, is that in rockets the Driver energy must be propagated through vacuum to the target. For terrestrial powerplants, energy propagation over a distance is also desired, but this can be either through vacuum or an atmosphere depending upon the needs of the Driver.

A number of different Driver technologies are being developed for ICF powerplants, and it is not yet clear which will ultimately triumph. Let's review the leading contenders, measuring their suitabilities for rocket use. The candidates may be split into two classes, those which transmit energy via particle beams and those which use lasers. Other options, such as high speed macroparticles have been proposed, but will not be a near term factor.

Charged particle Drivers are attractive because they offer high efficiency. A number of accelerator designs using particles ranging from electrons to heavy ions have been proposed, and should provide efficiencies of 25% or more.[9] The potential difficulty with using particle beams lies with focusing high fluxes of charged particles onto a small target. The flux required for a given species depends upon the energy carried by each particle, which is in turn determined by its range in the target. Representative values are 200 MA of 1 Mev electrons, 40 MA of 5 Mev protons, or 20 kA of 10 Gev U^+ ions. Such large currents of electrons will clearly be more difficult to focus than the small currents of heavy ions.

At one time electron beams were considered for ICF Drivers. However, they are difficult to focus, and also generate bremsstrahlung X-rays as they deposit. These X-rays penetrate further into the pellet than the electrons, and by preheating it, make an efficient implosion difficult. For these reasons serious work on electron Drivers has ceased in the USA. Sandia National Laboratory switched its efforts to proton acceleration, using diode accelerators very similar to their previous electron ones. Proton beams avoid the preheat problems of electrons, and are easier to focus than electron beams. However, they cannot be focused through vacuum to a pellet at 10-20 meter distances. For a terrestrial reactor this is not a fatal problem, and transport mechanisms[12] through atmospheric channels look promising. This approach is not feasible for a rocket, and the only option appears to be neutralization of the accelerated proton beam with a comoving electron cloud, allowing ballistic transport to the target. This approach will require higher quality (more uni-directional) proton beams than are likely to be developed for channel transport, and its stability is not yet certain.[12] If the transport problem can be solved, light ion accelerators should be useful in rockets, since they are reasonably compact, and ought to operate at high temperatures.

There is considerable interest in continuing the progression from light to heavy particles. When using heavy ions, such as U^+, the required currents are small enough to allow ballistic focusing over large distances. Furthermore, the target deposition mechanism is favorable; not only are no energetic particles created that can cause preheat, but the deposition versus depth profile is not the usual decaying exponential. The deposition occurs over a finite range, and mostly at the extreme end of this range. This permits tamped energy deposition, which should drive a more efficient implosion than the conventional ablation processes.[13] Two concepts have been studied, using conventional particle accelerator technology, and promising efficiencies of 20-30%.[9] The first uses RF linacs, and because these are low current devices, accumulates the ions in storage rings before extracting them, further compressing the pulse length with induction linacs, and focusing onto the target. The second system uses only induction linacs, which simultaneously accelerate the ions, and compress them to a short pulse-length beam. The problem with these approaches is that the Drivers are physically large and massive[14,15]. The existing designs have sizes in the 5-10 km range, and masses over 10,000 tons. While their costs appear competitive for ICF powerplants, their mass is not acceptable in a rocket. A number of unconventional approaches to heavy ion acceleration have been proposed which offer much smaller Drivers, an example of these is the IFA.[12] This scheme uses collective effects to accelerate U^{+60} ions over short distances. However, ballistic transport of such highly charged ions is no longer possible, and the aforementioned electron neutralization techniques must be developed. Since the more conventional accelerators appear adequate for powerplants, it is doubtful that collective accelerators will be developed for ICF.

The charged particle Drivers which are being developed for terrestrial ICF appear too massive for use in rockets. They are however not the only options being pursued. When the ICF program was started, the Drivers used were lasers, and these continue to dominate the program. Because of this head start, even if systems such as heavy ion accelerators are eventually used in powerplants, laser Drivers will have been developed for research, and probably pilot plants. Hence they will be available for use in rockets.

The advantage of lasers for ICF is that they are easily focusable onto targets at the required power levels. The difficulty lies in building large scale systems at high efficiency and low cost. Another problem which has proved troublesome is the effective coupling of the laser light to a pellet implosion. The interaction of high intensity coherent light with a plasma is not simple. A variety of processes exist that can backscatter light, reducing the absorption, and which can convert some of the absorbed energy into high energy electrons, which preheat the core of the pellet and spoil the implosion.[16] These effects are reduced for low wavelength lasers, and appear tolerable in the $\lambda \lesssim \frac{1}{3}\mu$ regime. A large number of laser systems have been proposed for ICF over the years. We will discuss the following 4 systems:

Free electron lasers are a new Driver option for ICF.[16] An FEL extracts energy from a high energy electron beam in the presence of a spatially oscillating magnetic field.[17] With proper design, this extraction should reach efficiencies of $\approx$ 40%. When combined with Linac or Betatron electron beam generation at $\approx$ 50%, the attrac-

tion of an FEL for ICF is clear. It offers short wavelength light (250nm), at system efficiencies near 15%. The advantages and drawbacks of an FEL Driver for a rocket can be illustrated by assuming an induction linac electron source. This accelerator technology is being actively pursued in the USA for high current, high beam quality applications, and will most likely be that used for any ICF Driver. The radiator mass for a rocket should be small; not only is the Driver efficiency high, but the heat can be generated at high temperatures. Energy not extracted from the electron beam can be dissipated in a very high temperature beam dump, while accelerator heating in conductors and iron core inductors can occur at temperatures of 600-700 °K. The problem is the same as with heavy ion accelerators, the Driver mass is large. In order to reach their high efficiencies, the inductors employ high permeativity cores. Scaling of current electron beam induction linacs yields a mass of over 2000 tons in the inductor cores alone.

CO_2 lasers are being pursued at the Los Alamos National Laboratory. They currently operate at pulsed efficiencies of $\approx 2\%$, but improved systems should reach values of 5-10%.[18] The primary difficulty facing CO_2 for ICF, is that it is a very high wavelength laser, $\lambda = 10.6\mu$. Accordingly, the laser energy is hard to efficiently couple into an implosion. Proposals have been made[9] for using vacuum or self generated magnetic fields to insulate the pellet core from energetic electrons. The technical feasibility of CO_2 driven ICF remains in doubt, which will presumably be resolved after the Antares laser at LASL becomes operational. For rocket use, even if a CO_2 Driver proves feasible and is developed, its low operational temperatures (generally 350-400 ^oK) will result in large heat rejection masses.

The most commonly used driver system in ICF research today is Nd:glass.[18] This laser generates short pulses of 1.06 μ light, which can be efficiently converted to $\frac{1}{2}$ or $\frac{1}{3}\mu$. However, because the existing lasers operate with very low efficiencies and rep rates, it is widely believed that this class of lasers will be useless in powerplants.[9] This view has been challenged in a recent review of rare earth doped solid state lasers.[19] The rep rate limits come from heat removal problems, which will be relaxed by using thin slabs rather than the current thick rods, by using high conductivity crystalline hosts instead of glass, and by increasing the laser efficiency. The laser efficiency can be increased by more effectively matching the absorption profile of the rare earth ions to the pumping source, by shortening the pump time compared to the upper state decay time, and by operating with longer laser pulses. If current flash lamp pumping sources are retained, a combination of longer lived lasing species and recycling of unused pump photons might allow efficiencies in the 10-20 % range. An alternative approach employs laser diode pumping, with very high conversion to the upper laser state of the rare earth ion. If these hoped for improvements materialize, then due to the current leading position of solid state lasers in ICF research they may *become a powerplant Driver. The energy storage density of* an efficient solid state laser will be 0.15-0.25 $J\,cm^{-3}$, which allowing for extraction losses translates to a mass of about 40 tons for the Driver of our rocket. This is acceptable, but the heat rejection masses are more troublesome. The gain of Nd lasers falls rapidly in the 400-500 °K regime. The projected future lasers will also suffer at elevated temperatures; thermal conductivity falls, upper state quenching increases, lower state population increases, and laser diode efficiency falls. Achieving an acceptable ηT^4 with solid state lasers will be considerably more difficult than increasing η itself.

Rare gas halides form a class of gas lasers invented long after the Nd:glass and CO_2 systems. A molecule such as KrF^* is formed, which is bound only in an electronically excited state. At moderate photon fluxes, $\approx 1\ MJ\,cm^{-2}$, the molecule lases before its natural decay into an unbound lower state. The KrF^* laser operates in the UV at 248 nm, and has, in separate experiments, been operated at 12% efficiency[20] and multi-kilojoule pulses. While the wavelength and efficiency of KrF^* makes it an attractive ICF Driver, it efficiently delivers only fairly long laser pulses, $\gtrsim 0.5\mu sec$. These long pulses can be efficiently compressed to the 10 ns sized ones required, using either Raman or pulse stacking techniques. KrF^* appears attractive for an IFR Driver since along with acceptable mass and efficiency, high temperature operation should be possible; it is a gas laser with no effective lower state.

Predicting which of the Drivers discussed above, or the myriad others also under consideration, will finally become adopted as the dominant ICF Driver is difficult. The issue will be decided on political, technical, and financial grounds with essentially no concern for the Driver's usefulness in rockets. From the above summaries, the KrF^* laser seems to be the most promising for an IFR. While the dominant US effort, for largely historical reasons, is centered upon Nd, CO_2, and light ions, there is substantial interest in KrF^* for ICF and other applications. A large KrF^* amplifier, 20 kJ, should be operating at Los Alamos within a year.[21] By using aperature combination and pulse compression techniques,[21] this module serves as the basic building block of an ICF Driver. Whether or not KrF^* is employed as a terrestrial ICF Driver, the technology base should exist to enable its use in a rocket. Accordingly, I have chosen it as the Driver in this rocket design.

The formation and lasing of KrF^* is a complex operation, and elaborate models have been developed to simulate these lasers.[20,22] Basicly, a gas mixture containing Ar, Kr, and F_2 is pumped by energetic electrons. As these slow down, their energy is spent forming rare gas ions and excited atoms. Both the excited neutrals and the ions then undergo reactions with either F_2 or F^- which lead to the formation of KrF^*, with an energy efficiency of $\approx 25\%$. Some of the KrF^* is lost via either quenching or decay before it can be lased. The laser photons that are created can be lost via absorption by F_2, F^-, Kr_2^+, or a host of other absorbing species. In order to predict the behavior of $\eta(T)$, I have developed a computer model similar to those mentioned above. Since most experimental determination of kinetic rates has occured at room temperature, the *correct extrapolation to higher temperatures is not* always clear. I believe that important processes such as ionic formation rates, and the vibrationally dependent molecular photo cross-sections are treated correctly, but most other rates are simply scaled kineticly. The basic trends shown

by this code are as follows. As T goes up, the KrF^* formation shifts to the neutral channels since the ionic rates drop. This does not significantly decrease the amount of KrF^* formed. The quenching rates increase weakly with temperature, and the the gain cross-section falls slightly, but for a saturated system the decrease in lasing is small. The primary effect of increased temperature appears to be increased absorption. The F^- absorption increases, since F^- removal by ionic recombination falls as T increases. Absorption by species such as Kr_2^+ and Kr_2F^* increases due to thermal population of higher vibrational levels. Hence, the laser efficiency falls with increasing temperature. This decrease is considerably weaker though than the T^4 improvement in radiator area.

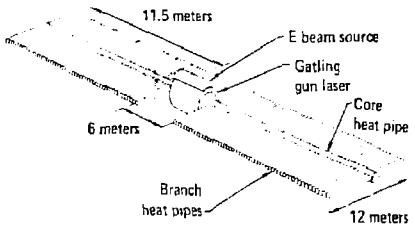

Fig. 3 Laser Module

The mass of the Driver used in this study is dominated by that of 200 laser amplifiers, one of which is shown in Fig. 3. Each module consists of a rotating cylinder containing the lasers, and a nonrotating heatpipe radiator. The laser gas is a mixture of Ar, Kr, and F_2, although at a lower density, $1.4 \times 10^{19}\ cm^{-3}$, and higher Kr fraction, 28%, than is normally used for these lasers. At the start of each pulse the gas is at a temperature of 1000°K, although this rises as electron energy is deposited. The laser operates with an intrinsic efficiency of 9%, but the difficulties of transporting electrons through the outer wall of the cylinder lower this to 6%. There are 5 laser buckets occupying the outer rim of the cylinder. Each is pumped as it passes the electron diode, a rate of 10 Hz. Between pulses the heated gas at the rim is bouyantly interchanged with the cooler gas in the interior of the cylinder. From here, its heat is transferred into corotating finned heatpipes. These employ a Na fluid, whose vapor is sent into the nonrotating core heatpipe of the radiator. Liquid return is via arteries in the core pipe, with wicked brush transfer to the finned heatpipes inside the cylinder. The actual radiator surface is the outer wall of the branch heat pipes. Because of thermal resistance, the actual radiating temperature is only 900°K. Each of these modules has a laser related mass of 520 kg, most of which resides in the cylinder walls and the optical windows. The radiators have an individual mass of 435 kg, 85% of which is in their walls.

The difficulties associated with high rep rate lasing and subsequent heat rejection, forced the use of two complete laser systems. Each contains 100 of the above modules, and fires at a 50 Hz rate. This alternative proved less difficult than designing higher performance modules. The amplifier modules are combined structurally and optically. Their connecting truss requires 12 tons; while the optical system to combine and pulse-stack the individual beams takes 6 tons. The oscillator system that is used to optically seed the amplifiers has a higher specific mass than they do, so has an 11 ton mass.

The laser Driver requires 33 MJ of energy per pulse. This energy is obtained from the thrust chamber; as induction coils are excited by the expansion of a pellet within the magnetic fields of the nozzle. This energy must be transported back to the Driver, via transmission lines, and stored there to wait for the next required laser firing, a period of 10 ms. In order to allow for pellet or laser misfires, we will store enough energy for several shots. Rotating machinery, such as the Compulsator[23], is capable of storing energy at low specific mass and with extraction times of $\approx$ 1 ms. This is adequate for the bulk energy store, but is too slow to directly pump a KrF^* laser. During the inter-pulse period, energy will be transferred into a capacitor array, from which it can be rapidly extracted to generate the $\frac{1}{2}$ μsec electron pulses which pump the laser. Unfortunately, capacitors are traditionally a mass intensive way to store energy. The current limits[24] of $\approx 0.5\ J\,gm^{-1}$ are not attractive for an IFR. By using vacuum dielectrics, the specific mass of capacitors can be greatly lowered at the expense of a similar increase in specific volume. For terrestrial use this tradeoff is not profitable, so there is little experience with large vacuum capacitors. For this study, we've assumed that the transmission line and capacitors each use vacuum dielectrics, and alloted masses of 5 and 25 tons respectively to these components. The rotating long-term energy store, by contrast, holds more energy and has a 12 ton mass.

Vehicle Summary

As can be seen from the mass breakdown in Table 3, the Driver and thrust chamber account for most of the mass of this inertial fusion rocket design. Various other components are also necessary, although they will not have much effect on the mass of the rocket. Let's briefly discuss some of these systems.

A neutron and γ-ray shield is placed on the vehicle axis at a location 20 meters away from the microexplosion. This shield consists of a cylinder which subtends a 3° half-angle in order to protect the payload region, and a thin fin which protects the thrust chamber radiators. These shields provide protection from direct shine, but a small radiation flux will bypass them by scattering out of the shield-coil. The magnet which deflects the plasma jet away from the rocket structure is placed directly behind this payload shield.

In order to reach the designated microexplosion point, a pellet must travel from the protection of the payload shield during the inter-pulse time. This requires that it

have a speed of 2 $km\ sec^{-1}$; which it will be given either by a magnetic accelerator[7], or by laser ablation. Extreme precision in target placement is not required, since the laser optics will be active and be designed to fire at the actual pellet location. In practice, slightly off-axis pellet explosions are probably the thrust vector control method which will be used.

At present, pellet costs are dominated by fabrication rather than fuel procurement. This situation must change when ICF leaves the research phase, and is used for powerplants or for rockets. Obviously, automated factories will be essential, and some preliminary studies of such plants have begun.[25] We have not attempted to design such a facility, but doubt that it will be massive. The tritium required for pellet ignition will be removed from the Li coolant loop at the thrust chamber radiator. It is then piped back to the factory, which will be located near the payload region.

The mass of the fusion pellet is often augmented by extra propellent mass. As is discussed in the next section, this is done to generate more thrust. In general, this propellent mass will dominate the fuel mass. In principle, this propellent can be any element, although my pellet-nozzle calculations have employed D_2. Assuming this choice is adopted, then for the Cargo missions in which the rocket will usually be employed, the fuel tankage requirement will be for ≈ 650 tons of D_2. Since this is a large scale system, and is subject to loads of only $\lesssim 0.1$ gee, 16 tons should be sufficient for tankage.

The vehicle drive will be turned-off for long periods of time, both between missions and during coasting sections of the trajectories. An auxiliary nuclear fission reactor will be provided to provide hhousekeeping power during these intervals, and to restart the propulsion system. A restart involves recharging the Driver energy banks, and reheating the laser gas. A 1 MW reactor with a mass of ≈ 5 tons will be adequate for these tasks.

Table 3 Vehicle Mass Summary

Driver	Tons
Lasers	110
Radiators	92
Optics, Structure	18
Energy Handling	42
	262
Thrust Chamber	
Shield-Coil	126
Heat Rejection	40
	166
Overhead	
Payload Shield	17
Fuel Tank	16
Reactor	5
Truss	20
	58
Total	486

The vehicle is tied together by a truss, which also transmits the vehicle thrust from its origin at the shield-coil, up to the payload. There are 8 primary thrust-bearing members. As with the Li-carrying heat-transfer pipes, they remain shadowed by the shield-coil until reaching the inner edge of the thrust chamber radiator, 50 meters from the microexplosion. At this location they are laterally tied together by a structural ring, and then fan out toward the Driver radiating array. Upon reaching this site, the truss no longer has circular symmetry, but instead is biased towards the radiating plane of the rocket. The thrust-bearing members are hollow pipes, and are tied together by a lateral truss in order to avoid buckling. As can be seen from the mission examples in Tables 4 and 5, the maximum vehicle thrust will be $\approx 3 \times 10^{11}$ *dyne*. The 20 ton truss can handle a 5×10^{11} *dyne* thrust.

Vehicle Performance

Having discussed the design of an inertial fusion rocket, let's see how well it performs.

As is the case with other advanced space-based rockets, an IFR can be characterized by the ratio of its maximum exhaust power to the mass of its powerplant, and by the maximum exhaust velocity at which it can expell propellent. The power-to-mass ratio is ultimately bounded by heat rejection from the Driver and the thrust chamber, but in practice is further degraded by the direct mass of these two systems. The maximum exhaust velocity that can be attained is upper bounded to $2.6 \times 10^9\ cm\ sec^{-1}$ by the specific energy available from fusion. In practice, this is degraded by the inefficiency of the nozzle, the loss of energy to neutrons and γ-rays, and most importantly by the fraction of the pellet mass used to implode the fuel. The relative importance of these two constraints depends upon the mission the rocket is performing.

For interstellar travel, the large distances demand that the rocket reach speeds which are at least $10 - 20\%c$ that of light. This is greater than our upper bound on exhaust velocity; so fuel loadings are large, and primary emphasis must be placed on raising the exhaust speed. Minimum powerplant mass and low tritium-inventory pellets, are not essential for an interstellar IFR. Instead, the vehicle design will concentrate on raising the nozzle efficiency, while the pellet designer must implode and burn as much of the fuel as possible.

This study has concentrated on a nearer term mission for inertial fusion rockets, i.e., interplanetary propulsion. This was done because it will be the initial application, and because an IFR can do a very good job at this task. For interstellar propulsion, an IFR may be the best presently known option, but in absolute terms it leaves a lot to be desired. Hopefully, by the time we build an interstellar rocket, it will be something better than an inertial fusion rocket.

For interplanetary travel, the capability of an IFR is limited more by its power-to-mass ratio, than by its ex-

haust velocity. The limitation on exhaust power translates into a bound on the product of exhaust speed "w" and acceleration "a", i.e., on aw. While a large value of w will eventually enable the rocket to reach a high speed, the low a means that doing so takes up a lot of time and distance. When the goal is to travel a given distance "D" as quickly as possible, the optimum technique involves accepting a lower w value in exchange for higher acceleration. This dialing of w can be accomplished in an IFR by placing excess propellent mass outside of the fusion pellet. The extra material lowers the exhaust velocity of the pellet, while increasing its impulse. Pellet-nozzle expansion calculations have been performed for different overall pellet masses, and show no change in nozzle efficiency.

We have used three models, of increasing sophistication and opacity, to analyze the performance of this IFR. The first is the classical power-limited model, in which gravity and exhaust velocity limits are neglected. This case is easy to solve, and indicates the pertinent scaling and operational modes. Next, the w constraint is included. The resulting zero-gee motion can also be analytically solved, but in a less useful form. This solution is then used as the starting point when numerically solving the 2D problem in which solar gravity is included along with the w and aw constraints.

By neglecting solar gravity and vehicle exhaust velocity limits, we gain a simple insight into the performance capabilities of an IFR. Suppose one wishes to travel a distance "D" in time "T", starting and stopping at rest. The rocket has an initial mass of "M_0", of which the powerplant accounts for a fraction "β" and is characterized by a power-to-mass ratio of "η". The optimum tradeoff between a and w occurs for the time dependent acceleration:

$$a(t) = \frac{12D}{T^3}\left(\frac{T}{2} - t\right), \qquad 0 \le t \le T \tag{1}$$

The payload fraction "λ" can be shown to be given by

$$\lambda = \frac{\beta}{\alpha + \beta} - \beta, \qquad \alpha = \frac{6D^2}{\eta T^3} \tag{2}$$

Note that D, T, and η appear only in the dimensionless parameter α. The trip time is seen to vary with the $\frac{1}{3}$ power of distance, and with the inverse cube root of the power-to-mass ratio. There are two interesting operational modes suggested by Eq. 2. The "VIP" mode yields the shortest possible trip time, but a vanishing payload. For this mode

$$D^2 = \frac{\eta T^3}{6}(1 - \beta) \tag{3}$$

For economical operation, one is willing to accept a longer trip time in exchange for a large payload fraction λ. The "Cargo" mode results from maximizing the payload throughput λ/T by optimizing over T and the choice of β. This optimum occurs at $\alpha = \frac{1}{16}$ and $\beta = \frac{3}{16}$, resulting in a payload fraction $\lambda = \frac{9}{16}$ and a fuel fraction of $\frac{1}{4}$. For this mode

$$D^2 = \frac{\eta T^3}{96} \tag{4}$$

In Table 4 we demonstrate the VIP mode capabilities of this rocket, and show Cargo performance in Table 5. For purposes of comparison, the VIP mode numbers assume the same powerplant fraction, $\beta = \frac{3}{16}$, which is optimal for cargo carrying; so the payload of the Cargo mission is swapped for more fuel in the VIP mission. The rocket exhaust power and exhaust velocity are given by

$$P = \nu E_K f_T^2, \qquad w = f_T\sqrt{\frac{2E_K}{m_p}} \tag{5}$$

For the current design, the nozzle efficiency f_T is 0.65, so the power P is 54.1 GW. Using the powerplant of Table 3, we find a power-to-mass of 110 $W\,gm^{-1}$. The examples illustrated in Tables 4 and 5 span the range of solar system missions; Martian close approach to show high acceleration capability, Pluto transit to show the opposite extreme, and an average Jupiter mission. The Tables list the distance, trip time, maximum speed, maximum acceleration, the exhaust speed at beginning and end, and the overall pellet mass at beginning and end.

Table 4 VIP Missions

		Mars	Jupiter	Pluto
D	(AU)	0.6	5.2	39.5
T	(day)	9.4	39.8	153.9
v_{max}	$(km\,sec^{-1})$	165	339	667
a_{max}	$(cm\,sec^{-2})$	51.1	39.5	20.1
w_0	$(km\,sec^{-1})$	52	104	205
w_T	$(km\,sec^{-1})$	271	557	1095
m_0	(gm)	422	100	26
m_T	(gm)	14.8	3.5	0.91

Table 5 Cargo Missions

		Mars	Jupiter	Pluto
D	(AU)	0.6	5.2	39.5
T	(day)	22.2	93.6	362
v_{max}	$(km\,sec^{-1})$	70	144	284
a_{max}	$(cm\,sec^{-2})$	14.7	7.14	3.69
w_0	$(km\,sec^{-1})$	281	577	1135
w_T	$(km\,sec^{-1})$	375	770	1513
m_0	(gm)	13.8	3.3	0.85
m_T	(gm)	7.8	1.8	0.49

The potential of this IFR for solar system propulsion is graphically illustrated by the trip times shown in Tables 4 and 5. A quick trip to Mars can be made in 9 days, while even in Cargo mode, Pluto can be reached in a year. In Cargo mode, the rocket can deliver 1500 tons per mission, while the VIP method still permits delivery of $\approx$ 50 ton payloads.

While enlightening, the above analysis is incomplete. The acceleration profile of Eq. 1 requires a zero acceleration and infinite exhaust velocity at the midpoint of the trajectory. Hence, the exhaust speed constraint will be violated during these trajectories. This will certainly occur in the middle of the trips, and for longer missions can occur throughout the journey. When a limitation on w is imposed on the trajectory optimization problem, its solu-

tion is no longer as transparent as Eq. 2; but analytic results can still be derived. The optimum trajectories consist of mixtures of three types of arcs. The beginning and end of a mission may or may not contain a linear acceleration, variable w, arc similar to that of Eq. 1. All missions contain an interior coasting arc, sandwiched between two arcs using the maximum w. In Table 6, I compare the final mass fractions for the Jupiter mission, as calculated both without a w limit, and with a bound of 600 $km\ sec^{-1}$. The final mass includes payload and powerplant, so the $T = 40\ day$ mission is not possible when the w limit is imposed. As expected, the initial analysis is always optimistic, with a larger error for the long trip time missions.

Table 6 Jupiter Mission

T	w free	w limit
110	0.829	0.732
110	0.785	0.702
90	0.727	0.662
80	0.652	0.606
70	0.556	0.545
60	0.441	0.41.
50	0.314	0.284
40	0.190	0.168

The thrust accelerations of Tables 4 and 5 are considerably larger than the solar gravitational pull of 0.6 $cm\ sec^{-2}$ at the Earth's orbit. However, when traveling between planets a ship does not start and stop at rest, but instead must match the planetary velocities. For this reason, and the fact that some trajectories can pass close to the Sun, I have considered the 2D problem. In this case, planetary orbits were assumed circular, and the vehicle is subject to its own thrust as well as solar gravity. The optimum trajectories are found numerically, using primer vector theory with an initial starting guess provided by the zero-gee model just discussed.

I have compared the above zero-gee results (with the w limit), to 2D ones which included solar gravity. The effects on payload fraction were as expected; payload went up when the planets were approaching each other, and down when they were receeding. But overall there was little change. To the eye, the trajectories of an IFR look like those of a solar system rocket should; straight lines between source and destination!

Prospectus

Inertial confinement fusion is now being vigorously pursued because of its potential for terrestrial powerplants. Its implications for space propulsion are even more profound. An inertial fusion rocket can carry kiloton payloads to any point of the solar system in less than a year.

The pacing item in the attainment of such a rocket remains the demonstration of ICF. The current status of pellet experiments, and the imminent completion of several pellet "Drivers", makes it likely that the scientific feasibility of inertial fusion microexplosions will be demonstrated by the end of this decade. Once this is done, the development of fusion rockets can proceed both in parallel with, and independently of, the powerplant effort. For a rocket, the most important component yet to be developed, is, as with terrestrial ICF, the Driver. The features which are uniquely required for a rocket; i.e., a high temperature excimer or solid-state laser, or a low mass particle accelerator, can be pursued inexpensively due to the modular nature of high performance Drivers. Confidence in system integration and full-scale Driver performance, will derive from the terrestrial ICF program. Items such as automated pellet factories are required for both applications, and will be developed by whichever program needs them first. Other advances in space technology will be important to incorporate into an IFR. Most useful will be advanced high temperature radiators, either using heatpipes or liquid droplets, and low mass capacitors, probably using vacuum dielectrics. But this work should not present major impediments to the development of an inertial fusion rocket.

It thus appears likely, that within the next 20-30 years, we can achieve a transport capability which allows us complete and rapid transit throughout interplanetary space.

References

1. A.R. Martin, A. Bond, "Nuclear Pulse Propulsion: A Historical Review of an Advanced Propulsion Concept," *Journal of the British Interplanetary Society*, Vol. 32, 1979, pp 283-310.
2. J.H. Nuckolls, *Internal technical memo, Lawrence Livermore National Laboratory*, 1961.
3. G.M. Benson, *Internal technical memo, Lawrence Livermore National Laboratory*, 1962.
4. K. Boyer, J.D. Balcomb, "System Studies of Fusion Powered Pulsed Propulsion Systems," *AIAA Paper, 71-636*, 1971.
5. F. Winterberg, "Rocket Propulsion by Thermonuclear Micro-Bombs Ignited With Intense Relativistic Electron Beams," *Raumfahrtforschung*, Vol. 5, Sept.-Oct 1971.
6. R.A. Hyde, L.L. Wood,Jr., J.H. Nuckolls, "Prospects For Rocket Propulsion with Laser-Induced Fusion Microexplosions," *AIAA Paper, 72-1063*, 1972.
7. A.R. Martin, Ed., "Project Daedalus," *Journal of the British Interplanetary Society*, Suppl. Vol. 1978.
8. J.H. Nuckolls, "The Feasibility of Inertial Confinement Fusion," *Physics Today*, Vol. 35, Sept. 1982, pp 24-31.
9. D. Keefe, "Inertial Confinement Fusion," *Ann. Rev. Nucl. Part. Sci.*, Vol. 32, 1982, pp 391-441.

10. R.A. Haas, "General Principles of Inertial Confinement Fusion," *Lawrence Livermore National Laboratory, Report UCRL-88709*, 1983.

11. E.F. Plechaty, J.R. Kimlinger, "TARTNP: A Coupled Neutron-Photon Monte-Carlo Transport Code," *Lawrence Livermore National Laboratory, Report UCRL-50400, Vol. 14*, 1976.

12. C.L. Olson, "Ion Beam Propagation and Focusing," *Journal of Fusion Energy*, Vol. 1, 1982, pp 309-339.

13. R.O. Bangerter, D.J. Meeker, "Ion Beam Inertial Fusion Target Designs," *Lawrence Livermore National Laboratory, Report UCRL-78474*, 1976.

14. "HIBALL—A Conceptual Heavy Ion Beam Driven Fusion Reactor Study," *Institut für Neutronenphysik und Reaktortechnik, Report KfK 3202, UWFDM-450*, 1981.

15. A. Faltens, D. Keefe, "Ion Induction Linacs: Reference Design and Proposed Test-Bed," *Proc. Heavy-Ion Fusion Workshop, Berkeley, 1975*, Law. Berk. Lab. *Report LBL-10301*, 1980, pp 157-181.

16. D. Prosnitz, "Free Electron Lasers," *Lawrence Livermore National Laboratory, Report UCRL-50021-80*, Vol. 3, 1980, pp 8-55-8-60.

17. P. Morton, "Free Electron Lasers," *IEEE Trans. on Nuclear Science*, Vol. NS-28, 1981, pp 3125-3129.

18. J.F. Holzrichter, D.Eimerl, E.V. George, J.B. Trenholme, W.W. Simmons, J.T. Hunt, "High Power Pulsed Lasers," Journal of Fusion Energy, Vol. 2, 1982, pp 5-45.

19. J.L. Emmett, W.F. Krupke, J.B. Trenholme, "The Future Development of High-Power Solid State Laser Systems," *Lawrence Livermore National Laboratory, Report UCRL-53344*, 1982.

20. T.H. Johnson, A.M. Hunter,II, "Physics of the Krypton Fluoride Laser," *Journal of Applied Physics*, Vol. 51, 1980, pp 2406-2420.

21. G.H. Canavan, R.O. Hunter,Jr., A.M. Hunter,II, "Development and Application of Advanced High Energy Lasers," *Los Alamos National Laboratory, Report LA-UR 83-202*, 1983.

22. C.B. Edwards, F. O'Neill, "Computer Modelling of E-Beam-Pumped KrF Lasers," *Laser and Particle Beams*, Vol. 1, 1983, pp 61-95.

23. R.J. Foley, W.F. Weldon, "Compensated Pulsed Alternator," *Lawrence Livermore National Laboratory*, Oct. 1980.

24. R.D. Parker, "Energy Storage Capacitors of Very High Energy Density," *IEEE Trans. on Parts, Hybrids, and Packaging*, Vol. PHP-13, 1977, pp 156-165.

25. J.W. Sherohman, W.R. Meier, "A Parametric Study of a Target Factory For Laser Fusion," *Lawrence Livermore National Laboratory, Report UCRL-84264*, 1980.

Work performed under the auspices of the U.S. Department of Energy by Lawrence Livermore National Laboratory under Contract W-7405-Eng-48.